

A second-order, perfectly matched layer formulation to model 3D transient wave propagation in anisotropic elastic media

Hisham Assi* and Richard S. C. Cobbold

Institute of Biomaterials and Biomedical Engineering, University of Toronto,
164 College Street, Toronto, M5S 3G9, Canada

Abstract

Numerical simulation of wave propagation in an infinite medium is made possible by surrounding a finite region by a perfectly matched layer (PML). Using this approach a generalized three-dimensional (3D) formulation is proposed for time-domain modeling of elastic wave propagation in an unbounded lossless anisotropic medium. The formulation is based on a second-order approach that has the advantages of, physical relationship to the underlying equations, and amenability to be implemented in common numerical schemes. Specifically, our formulation uses three second-order equations of the displacement field and nine auxiliary equations, along with the three time histories of the displacement field. The properties of the PML, which are controlled by a complex two-parameter stretch function, are such that it acts as near perfect absorber. Using finite element method (FEM) 3D numerical results are presented for a highly anisotropic medium. An extension of the formulation to the particular case of a Kelvin-Voigt viscoelastic medium is also presented.

Keyword: Perfectly matched layers; Elastic waves; Second order time-domain; Anisotropic media; viscoelastic media

Contents

1	Introduction	2
2	Background and materials	4
2.1	Elastic waves in solids	4
2.2	Complex coordinates stretching	5

**Email address:* hisham.assi@mail.utoronto.ca

3	Formulation of PML for elastic wave propagation	7
4	Numerical Methods and Results	9
5	Conclusion	14
	Appendix A PML for viscoelastic media	20

1 Introduction

Perfectly matched layers [1] are a well-developed method for simulating wave propagation in unbounded media enabling the use of a reduced computational domain without having to worry about spurious boundary reflections. Bérenger showed that by adding specific conductivity parameters to Maxwell’s equations, perfect matching and decaying of the propagating waves in the PML could be achieved [1]. An alternative method is to assume that the material contained within the PML is a uniaxial anisotropic media [2–4], generally referred to as the uniaxial PML approach. A third method, with greater generality and flexibility, is the complex coordinate stretching approach [5]. In fact, the conductivity parameter introduced by Bérenger [1] can be thought of as a damping parameter in a stretch function that transforms the spatial coordinate in the layer to the complex plane.

Subsequent to these electromagnetic wave applications, many PML formulations have been introduced for elastic wave propagation [6–12]. Amongst these, the split-field formulations that are typically described by systems of first order equations with double (for 2D) or triple (for 3D) the number of stress-velocity physical equations (nine equations in all for the 3D case) . Second-order formulations uses one physical field variable (usually the displacement) along with extra auxiliary variables that are typically needed to obtain the time-domain equations from the frequency-domain equations. Mathematically, it has been proven that certain second-order PMLs are strongly

well-posed, while the first-order type is only weakly well-posed [13–15].

There are other advantages for choosing second-order formulations. The second-order displacement elastic wave equation emerges directly from Newton’s second law [15], unlike the first-order stress-velocity elastic wave equation which introduces a new non-physical wave mode with zero velocity [10, 15]. Moreover, the second-order PML formulations are more readily implemented in common numerical schemes that are based on second-order displacement wave equations [16, 17]. However, deriving second-order PML formulations is less trivial than that for first-order ones, especially in the time-domain where many auxiliary variables are needed. The problem becomes more complex for the 3D modeling which would partially explain the dearth of second order formulations in 3D.

There have been a number of papers that describe the formulation of time-domain wave propagation in 3D fluid media using PMLs (see of example [18, 19]) but there are relatively few that address the same problem for anisotropic, inhomogeneous elastic media, especially those attempting a second-order formulation. In previous works [20, 21], the authors introduced a compact second-order time-domain PML formulations for the elastic wave equation in 2D which has only four auxiliary variable. Recently Lee and Shin [22] introduced an unsplit PML formulation for isotropic media or media with vertical axis of symmetry (VTI). Their 2D derivation was based on second-order elastic wave equations, and the final formulation followed closely the one given in Assi and Cobbold [20, 21]. It should be noted that the final form of the PML formulation, and not the way it was derived, that governs its robustness and other characteristics. Additionally, Lee and Shin extended their formulation to 3D VTI media for which they presented numerical results [22].

The purpose of this paper is to derive a time-domain second-order formulation to model elastic wave propagation in an unbounded three-dimensional general anisotropic

inhomogeneous solid. As will be seen the formulation results in a system of equations that are applicable throughout the computational domain. In the physical domain, the complex stretch function is simply set to unity. To demonstrate the application of our formulation, propagation from a spherical transient source embedded in a highly anisotropic medium (the mineral Olivine) is illustrated. Extension of the formulation to include a viscoelastic medium that can be represented by a Kelvin-Vogit model [23, 24], is presented in [appendix A](#).

2 Background and materials

2.1 Elastic waves in solids

Wave propagation in linear elastic solids can be described using Newton’s second law, along with Hook’s law and a linear approximation for the strain. These lead to the following second-order formulation of the elastic wave equation:

$$\rho \frac{\partial^2 u_i}{\partial t^2} - \sum_{j=1}^3 \frac{\partial}{\partial x_j} \left(\sum_{k,l=1}^3 C_{ijkl} \frac{\partial u_k}{\partial x_l} \right) = 0, \quad (1)$$

where $t \in \mathbb{R}^+$ is time, $\mathbf{x} \in \mathbb{R}^3$ is the space variable, $u_i(\mathbf{x}, t)$ are the components of particle displacement vector. Moreover, $\rho(\mathbf{x})$ is the solid mass density and $C_{ijkl}(\mathbf{x})$ are the components of the fourth order elasticity tensor with the following symmetry properties: $C_{ijkl} = C_{ijlk} = C_{jikl}$, and $C_{ijkl} = C_{klij}$. The source of energy that excites the elastic medium can be added as a load vector, $F_i(\mathbf{x}, t)$, to the right-hand side (RHS) of (1).

In general, the elasticity tensor, C_{ijkl} , has 81 components, but due to the above symmetries, the maximum number of independent parameters is 21. For the special case of isotropic solids, the elasticity tensor can be described by two independent parameters

such as the Lamé coefficients, $\lambda(\mathbf{x})$ and $\mu(\mathbf{x})$. In terms of these two coefficients, the elasticity tensor can be written as:

$$C_{ijkl} = \lambda\delta_{ij}\delta_{kl} + \mu(\delta_{ik}\delta_{jl} + \delta_{il}\delta_{jk}), \quad (2)$$

where δ_{ij} is the Kronecker delta function.

For the purpose of plane wave and Fourier analyses, the harmonic wave solutions of the following form:

$$\mathbf{u} = \mathbf{A} \exp [i(\mathbf{k} \cdot \mathbf{x} - \omega t)], \quad (3)$$

will be considered for the elastic wave equation as given by (1). In this equation, $\mathbf{A} \in \mathbb{C}^3$ is the constant amplitude polarization vector, $\mathbf{k} \in \mathbb{R}^3$ is the wavevector, $\omega \in \mathbb{C}$ is the angular frequency, and $i^2 = -1$.

2.2 Complex coordinates stretching

To obtain a PML formulation for a given wave equation, the complex coordinate stretching [5] can be expressed as a coordinate transform: $\mathbf{x} \mapsto \tilde{\mathbf{x}} : \mathbb{R}^3 \rightarrow \mathbb{C}^3$. Since $\tilde{\mathbf{x}} = \mathbf{x}$ in the physical domain and the PML region is assumed to be homogeneous, then $\tilde{\mathbf{x}}$ appears only in the form of spatial partial derivatives in the PDEs. Given a field variable u , then using the chain rule: $\frac{\partial u}{\partial x_j} = \sum_{k=1}^3 \frac{\partial u}{\partial \tilde{x}_k} \frac{\partial \tilde{x}_k}{\partial x_j}$, which reduces to $\frac{\partial u}{\partial x_j} = \frac{\partial u}{\partial \tilde{x}_j} \frac{\partial \tilde{x}_j}{\partial x_j}$ since \tilde{x}_j depends only on x_j . As a result, defining the complex stretch function by $s_j(x_j) = \frac{\partial \tilde{x}_j}{\partial x_j}$ suffices to perform transformation:

$$\frac{\partial}{\partial \tilde{x}_j} = \frac{1}{s_j(x_j)} \frac{\partial}{\partial x_j}. \quad (4)$$

The two-parameter complex stretch function introduced by Fang and Wu [25] in

their generalized PML (GPML) is adopted in this paper. This function is given by

$$s_j(x_j) = \alpha_j(x_j) \left[1 + i \frac{\beta_j(x_j)}{\omega} \right], \quad (5)$$

where the $\beta_j \geq 0$ is the damping parameter responsible for damping the propagating wave inside the PML. In this equation, the scaling parameter, $\alpha_j > 0$, is responsible for either stretching ($\alpha_j > 1$) or compressing ($0 < \alpha_j < 1$) the coordinate. It should be noted that in the physical domain, where $\tilde{x}_j(x_j) = x_j$, $\beta_j = 0$ and $\alpha_j = 1$.

Appropriate choices are now needed for the stretch function parameters $\alpha_j(x_j)$ and $\beta_j(x_j)$. Despite the absence of a rigorous methodology for their choice [9, 12], polynomial functions are often used as indicated below for the damping parameter:

$$\beta_j(x_j) = \begin{cases} 0 & \text{if } |x_j| < x_0 \\ \beta_{0_j} \left(\frac{|x_j| - x_0}{d} \right)^n & \text{if } x_0 \leq |x_j| \leq x_0 + d, \end{cases} \quad (6)$$

where d is the thickness of the PML, $2x_0$ is the dimension of the square physical domain centered at the origin, n is the polynomial order, β_{0_j} is a constant that represent the maximum values of β_j . The value of this parameter needs to be specified. It is helpful to express the value of β_{0_j} in terms of a desired amplitude reflection coefficient (R_j) caused by the reflection from the outer boundary of the PML. It can be shown that for normal incidence and assuming $\alpha_j = 1$,

$$h\beta_{0_j} = \frac{c_{\max}(n+1) \ln(1/R_j)}{2d}. \quad (7)$$

Quadratic polynomial, corresponds to $n = 2$, will be used in this work unless mentioned otherwise. Without loss of generality, the scaling parameter, α_j , is set to unity in this work. This parameter can be readily introduced back to any PML formulation that is

derived using the complex stretch function in (5), by replacing each $\partial/\partial x_j$ by $\partial/\alpha_j \partial x_j$ in the PDEs.

3 Formulation of PML for elastic wave propagation

With the help of the above background, our time-domain PML formulation can be introduced for the wave propagation in unbounded media. All parameters, namely, ρ , C_{ijkl} , β_j , and s_j , are assumed to be space dependent throughout the derivation leading to a variable-coefficient PML formulation. Since the stretch function also depends on the frequency, the derivation starts in the frequency domain.

First, we take Fourier transforms of the elastic wave equation (1), and then transform the spatial coordinates using complex stretching, $\mathbf{x} \mapsto \tilde{\mathbf{x}}$, as introduced in subsection 2.2. These steps lead to:

$$(-i\omega)^2 \hat{u}_i \rho = \sum_{j=1}^3 \frac{\partial}{\partial \tilde{x}_j} \left(\sum_{k,l=1}^3 C_{ijkl} \frac{\partial \hat{u}_k}{\partial \tilde{x}_l} \right), \quad (8)$$

where $\hat{\square}$ denotes the Fourier transform in time. The need to solve this differential equation along contours in the complex plane can be avoided by inverse transforming the complex-stretched coordinates back to the original spatial coordinates using (4). This is followed by multiplying the equation by $s_1 s_2 s_3$, leading to:

$$s_1 s_2 s_3 (-i\omega)^2 \hat{u}_i \rho = \sum_{j=1}^3 \frac{s_1 s_2 s_3}{s_j} \frac{\partial}{\partial x_j} \left(\sum_{k,l=1}^3 C_{ijkl} \frac{1}{s_l} \frac{\partial \hat{u}_k}{\partial x_l} \right). \quad (9)$$

Expanding $s_1 s_2 s_3$ according to (5) while assuming $\alpha_j = 1$, the left-hand side (LHS) of the above equation becomes:

$$\rho \left[(-i\omega)^2 + (-i\omega) (\beta_1 + \beta_2 + \beta_3) + (\beta_1 \beta_2 + \beta_2 \beta_3 + \beta_3 \beta_1) + \frac{\beta_1 \beta_2 \beta_3}{(-i\omega)} \right] \hat{u}_i. \quad (10)$$

Here, it is helpful to introduce the variable

$$U_i(\mathbf{x}, t) = \int_0^t u_i(\mathbf{x}, \tau) d\tau, \quad (11)$$

whose Fourier transform is given by $\hat{U}_j(\mathbf{x}, \omega) = \hat{u}_i(\mathbf{x}, \omega)/(-i\omega) + \pi \hat{u}_i(\mathbf{x}, 0)\delta(\omega)$. However, the second term vanishes since the stretch function (5) is not defined for the static case of $\omega = 0$ [12]. Consequently, substituting $\hat{u}_i = -i\omega \hat{U}_i$ in the last term of (10) and taking inverse Fourier transform ($-i\omega \Rightarrow \partial/\partial t$) of this, results in

$$\rho \left[\frac{\partial^2 u_i}{\partial t^2} + (\beta_1 + \beta_2 + \beta_3) \frac{\partial u_i}{\partial t} + (\beta_1 \beta_2 + \beta_2 \beta_3 + \beta_3 \beta_1) u_i + \beta_1 \beta_2 \beta_3 U_i \right]. \quad (12)$$

It should be noted that $s_1(x_1)s_2(x_2)s_3(x_3)/s_j(x_j) = \prod_{i \neq j} s_i(x_i)$, and hence does not depend on x_j , enabling the RHS of (9) to be written as:

$$\sum_{j=1}^3 \frac{\partial}{\partial x_j} \left(\sum_{k,l=1}^3 \frac{s_1 s_2 s_3}{s_j s_l} C_{ijkl} \frac{\partial \hat{u}_k}{\partial x_l} \right). \quad (13)$$

After some manipulations, it can be shown that

$$\frac{s_1 s_2 s_3}{s_j s_l} = 1 + \frac{\beta_1 + \beta_2 + \beta_3 - \beta_j - \beta_l + \frac{\beta_1 \beta_2 \beta_3}{-i\omega \beta_l}}{-i\omega + \beta_j} \quad (14)$$

At this point, we introduce the auxiliary variables, $w_{ij}(\mathbf{x}, t)$ such that their Fourier transform

$$\hat{w}_{ij}(\mathbf{x}, \omega) = \sum_{k,l=1}^3 \frac{\beta_1 + \beta_2 + \beta_3 - \beta_j - \beta_l + \frac{\beta_1 \beta_2 \beta_3}{-i\omega \beta_l}}{-i\omega + \beta_j} C_{ijkl} \frac{\partial \hat{u}_k}{\partial x_l}. \quad (15)$$

Multiplying the above equations by $-i\omega + \beta_j$ and taking its inverse Fourier transform

results in the following time-domain auxiliary equations:

$$\frac{\partial w_{ij}}{\partial t} + \beta_j w_{ij} = \sum_{k,l=1}^3 \left((\beta_1 + \beta_2 + \beta_3 - \beta_j - \beta_l) C_{ijkl} \frac{\partial u_k}{\partial x_l} + \frac{\beta_1 \beta_2 \beta_3}{\beta_l} C_{ijkl} \frac{\partial U_k}{\partial x_l} \right), \quad (16)$$

and the RHS of (9) becomes

$$\sum_{j=1}^3 \frac{\partial}{\partial x_j} \left(\sum_{k,l=1}^3 C_{ijkl} \frac{\partial u_k}{\partial x_l} + w_{ij} \right). \quad (17)$$

This concludes our derivation, so that the final second-order time-domain PML formulation for elastic wave propagation in three-dimensional anisotropic solid can be written as

$$\rho \left(\frac{\partial^2 u_i}{\partial t^2} + a \frac{\partial u_i}{\partial t} + b u_i + c U_i \right) = \sum_{j=1}^3 \frac{\partial}{\partial x_j} \left(\sum_{k,l=1}^3 C_{ijkl} \frac{\partial u_k}{\partial x_l} + w_{ij} \right) \quad (18a)$$

$$\frac{\partial w_{ij}}{\partial t} + \beta_j w_{ij} = \sum_{k,l=1}^3 \left(\tilde{C}_{ijkl} \frac{\partial u_k}{\partial x_l} + \check{C}_{ijkl} \frac{\partial U_k}{\partial x_l} \right) \quad (18b)$$

$$\frac{\partial U_i}{\partial t} = u_i, \quad (18c)$$

where $a(\mathbf{x}) = \beta_1 + \beta_2 + \beta_3$, $b(\mathbf{x}) = \beta_1 \beta_2 + \beta_2 \beta_3 + \beta_3 \beta_1$, $c(\mathbf{x}) = \beta_1 \beta_2 \beta_3$, $\tilde{C}_{ijkl}(\mathbf{x}) = (a - \beta_j - \beta_l) C_{ijkl}$, and $\check{C}_{ijkl}(\mathbf{x}) = (c / \beta_l) C_{ijkl}$.

4 Numerical Methods and Results

For our studies, the source of excitation was a 1 mm radius sphere, centered at the origin and embedded in an infinite 3D medium. To model the infinite medium we assumed a cubic physical domain of 2.0 cm³ that is centered at the origin and surrounded by a 2.0 mm PML. The boundary of the sphere was assumed to vibrate with a displacement,

whose normalized time-dependence is given by the first derivative of a Gaussian, i.e., by

$$u_0(t) = -\sqrt{2e} \pi f_0 (t - t_0) e^{-\pi^2 f_0^2 (t-t_0)^2}, \quad (19)$$

where f_0 is the dominant frequency and t_0 is a source delay time. All numerical experiments used $f_0 = 1$ MHz and $t_0 = 1$ μ s.

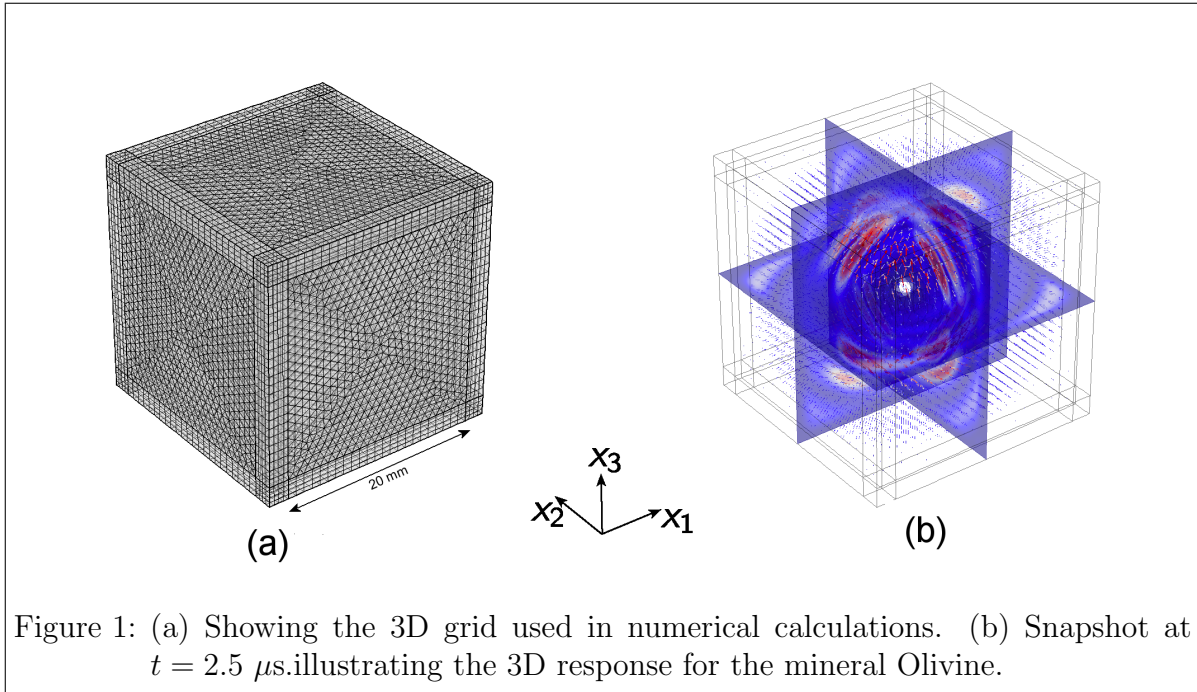
The simulations were performed using COMSOL with the second-order Lagrange finite elements employing a cubic mesh for the PML region and the default tetrahedral shape in the physical domain (see [Figure 1a](#)). For discussing the mesh dimensions and time discretization, it is helpful to define the minimum and maximum characteristic wave speeds associated with the medium by c_{\min} and c_{\max} . The mesh size is governed by the shortest wavelength of significance for the propagating pulse, i.e., by c_{\min}/f_c . Specifically, the mesh size was assumed to be given by

$$h_0 = \frac{c_{\min}}{N f_0}, \quad (20)$$

which for the second-order accurate finite elements used, corresponds to $2N$ degrees of freedom per wavelength. As illustrated in [Figure 1a](#), the mesh employed uses a PML whose thickness consists of just four elements. As will be seen this is sufficient to ensure virtually complete absorption of the various incident waves. For the time discretization, a second-order generalized alpha method, as defined by Chung and Hulbert [26], was used with $\rho_\infty = 0.75$. The step duration was $0.9h_0/c_{\max}$, which is just less than the time needed for the fastest wave to travel through the smallest mesh dimension.

To test the validity of our formulation and the accuracy with which our finite element simulations describe the propagating pulse, the exact solution for a monochromatic compressional wave caused by a 1-mm radius sphere whose surface vibrated normal to the surface [27] was used. The sphere was assumed to be embedded in an

unbounded isotropic solid (glass). By multiplying this monochromatic solution with the Fourier transform of equation (19) and then taking the inverse Fourier transform, the time-domain analytic solution was obtained. Good agreement with the numerically calculated response provided convincing evidence for the validity of our 3D formulation, though the results are not presented here.



To illustrate the application of our general formulation, we chose to present the results for a highly anisotropic medium. In particular, we chose to examine the 3D response when the above source, in (19), is contained within in a single crystal of olivine (Mn_2SiO_4). Olivine is a mineral with an orthorhombic structure and nine independent elasticity components whose measured parameters at $25^\circ C$ are given by [28, 29]: $c_{11} = 2.58$, $c_{22} = 1.66$, $c_{33} = 2.07$, $c_{44} = 0.45$, $c_{55} = 0.56$, $c_{66} = 0.58$, $c_{12} = 0.87$, $c_{13} = 0.95$, $c_{23} = 0.92$ Mbar. Unlike the isotropic case, fast and slow waves propagate in anisotropic solids even if the excitation is normal to the sphere's surface. Nevertheless, in order to observe a clearer presence of these different waves, we decided to to excite the medium

by vibrating the sphere's surface at 45° to the normal in the polar direction. Namely, the Dirichlet boundary condition at the surface of the sphere is set to:

$$\frac{1}{\sqrt{2}}(\hat{\mathbf{n}} + \hat{\mathbf{t}}_\phi) u_0(t), \quad (21)$$

where u_0 is defined in (19), $\hat{\mathbf{n}}$ is the normal unit vector, and $\hat{\mathbf{t}}_\phi$ is the tangential unit vector in the ϕ direction, and ϕ is the polar angle that varies from 0 to π away from the x_3 -axis. At $\phi = 90^\circ$ for example, $\hat{\mathbf{t}}_\phi$ is in the negative x_3 -direction, hence, the quasi-longitudinal wave is expected to be dominant on the x_1 - x_2 plane.

The results of the simulations are presented as density and vectors plots that represent the magnitudes and the directions of the normalized displacement field. While Figure 1b provides a snapshot of the propagating waves in a 3D format, such an image is difficult to interpret. The three sets of snapshots for three different planes, as shown in the nine panels of Figure 2, provides much more detailed information. These snapshots show 2D plots of the field on the three principal planes at $1 \mu\text{s}$, $2.2 \mu\text{s}$, and $3.5 \mu\text{s}$. The first column shows the displacement field on the x_1 - x_2 plane, wherein, as expected, the fast wave is dominant. Meanwhile, on the other two planes, the three waves; the quasi-longitudinal (fast) and the two quasi-shear (slow), are clearly present as shown in the $2.2 \mu\text{s}$ snapshots. At this time, the fast wave is being effectively absorbed by the PML, while the slow waves are being absorbed in the $3.5 \mu\text{s}$ snapshot.

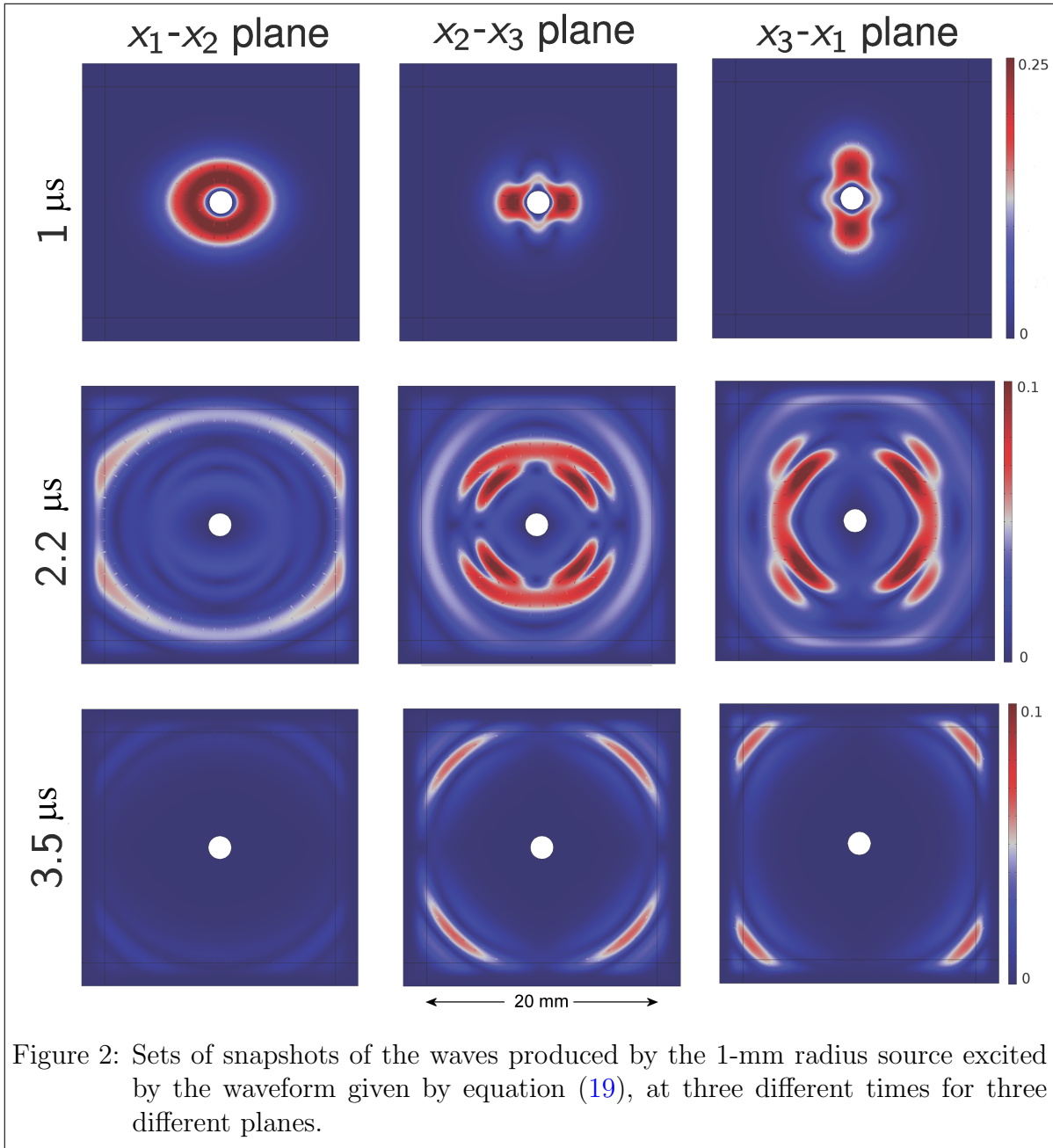


Figure 2: Sets of snapshots of the waves produced by the 1-mm radius source excited by the waveform given by equation (19), at three different times for three different planes.

The effectiveness of the PML to absorb all the incident energy can be obtained by looking at the manner in which the energy in the physical domain evolves over time. Since the total energy in the physical domain is the sum of the kinetic and potential

energy, it can be calculated from

$$E(t) = \frac{1}{2} \int_{\Omega} \left[\rho \sum_{j=1}^3 \left(\frac{\partial u_j}{\partial t} \right)^2 + \sum_{i,j,k,l=1}^3 C_{ijkl} \frac{\partial u_i}{\partial x_j} \frac{\partial u_k}{\partial x_l} \right] d\Omega. \quad (22)$$

Figure 3 shows that the total energy decays to a negligible level in less than 5 μs .

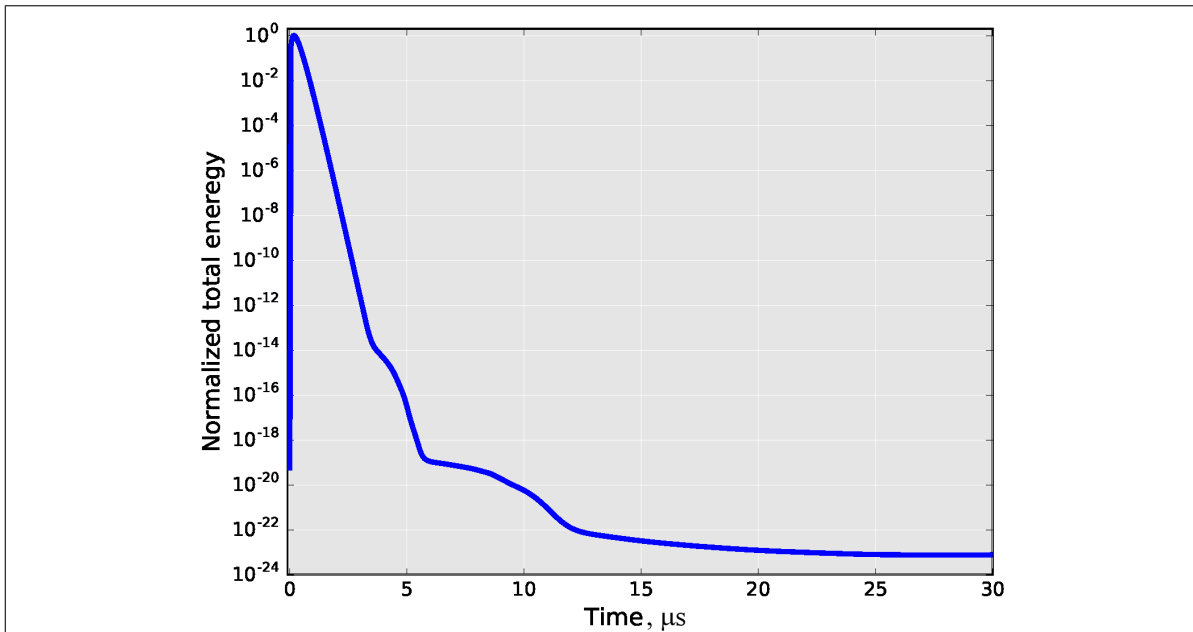


Figure 3: The decay of energy as calculated from (22) in the physical domain for the mineral Olivine showing that the PML acts as a near ideal absorber.

5 Conclusion

Using PML approach we have addressed the problem of wave propagation in an unbounded, linear anisotropic solid in three dimensions. A time-domain second order PDE has been derived using complex coordinate stretching. The advantages of our time-domain formulation is the fact that it covers the more general inhomogeneous anisotropic case using a small number of equations. Specifically, three second-order equations of the displacement field and nine auxiliary equations, along with the time

histories of the displacement field. This simplifies the problem and reduces the computational resources needed. Moreover, use can be made of a wider variety of second-order numerical schemes.

Acknowledgments

We wish to thank the Natural Sciences and Engineering Research Council (NSERC) for their support [grant number 3247-2012]. We also wish to thank Pooya Bidari from Ryerson University for drawing to our attention the importance of developing a viscoelastic 3D model.

References

- [1] J.-P. Bérenger, “A perfectly matched layer for the absorption of electromagnetic waves,” *J. Comput. Phys.*, vol. 114, no. 2, pp. 185–200, 1994.
- [2] Z. S. Sacks, D. M. Kingsland, and R. Lee, “A perfectly matched anisotropic absorber for use as an absorbing boundary condition,” *IEEE Trans. Antennas Propag.*, vol. 43, no. 12, pp. 1460–1463, 1995.
- [3] J. A. Roden and S. D. Gedney, “Efficient implementation of the uniaxial-based PML media in three-dimensional nonorthogonal coordinates with the use of the FDTD technique,” *Microwave Opt. Technol. Lett.*, vol. 14, no. 2, pp. 71–75, 1997.
- [4] S. D. Gedney, “An anisotropic perfectly matched layer-absorbing medium for the truncation of FDTD lattices,” *IEEE Trans. Antennas Propag.*, vol. 44, no. 12, pp. 1630–1639, 1996.
- [5] W. C. Chew and W. H. Weedon, “A 3D perfectly matched medium from modified maxwell’s equations with stretched coordinates,” *Microwave Opt. Technol. Lett.*, vol. 7, no. 13, pp. 599–604, 1994.
- [6] F. Collino and C. Tsogka, “Application of the perfectly matched absorbing layer model to the linear elastodynamic problem in anisotropic heterogeneous media,” *Geophysics*, vol. 66, no. 1, pp. 294–307, 2001.
- [7] F. Hastings, J. B. Schneider, and S. L. Broschat, “Application of the perfectly matched layer (PML) absorbing boundary condition to elastic wave propagation,” *J. Acoust. Soc. Am.*, vol. 100, no. 5, pp. 3061–3069, 1996.
- [8] F. H. Drossaert and A. Giannopoulos, “Complex frequency shifted convolution

- PML for FDTD modelling of elastic waves,” *Wave Motion*, vol. 44, no. 7-8, pp. 593–604, 2007.
- [9] W. C. Chew and Q.-H. Liu, “Perfectly matched layers for elastodynamics: A new absorbing boundary condition,” *J. Comput. Acoust.*, vol. 4, no. 4, pp. 341–359, 1996.
- [10] D. Appelö and G. Kreiss, “A new absorbing layer for elastic waves,” *J. Comput. Phys.*, vol. 215, no. 2, pp. 642–660, 2006.
- [11] K. C. Meza-Fajardo and A. S. Papageorgiou, “A nonconvolutional, split-field, perfectly matched layer for wave propagation in isotropic and anisotropic elastic media: stability analysis,” *Bull. Seismol. Soc. Am.*, vol. 98, no. 4, pp. 1811–1836, 2008.
- [12] S. Kucukcoban and L. F. Kallivokas, “Mixed perfectly-matched-layers for direct transient analysis in 2D elastic heterogeneous media,” *Comput. Meth. Appl. Mech. Eng.*, vol. 200, no. 1-4, pp. 57–76, 2011.
- [13] A. Deinega and I. Valuev, “Long-time behavior of PML absorbing boundaries for layered periodic structures,” *Comput. Phys. Commun.*, vol. 182, no. 1, pp. 149–151, 2011.
- [14] S. Abarbanel, D. Gottlieb, and J. S. Hesthaven, “Long time behavior of the perfectly matched layer equations in computational electromagnetics,” *J Sci Comput*, vol. 17, no. 1-4, pp. 405–422, 2002.
- [15] K. Duru and G. Kreiss, “A well-posed and discretely stable perfectly matched layer for elastic wave equations in second-order formulation,” *Commun. Comput. Phys.*, vol. 11, no. 5, pp. 1643–1672, 2012.

- [16] D. Komatitsch and R. Martin, “An unsplit convolutional perfectly matched layer improved at grazing incidence for the seismic wave equation,” *Geophysics*, vol. 72, no. 5, pp. SM155–SM167, 2007.
- [17] Y. Li and O. B. Matar, “Convolutional perfectly matched layer for elastic second-order wave equation,” *J. Acoust. Soc. Am.*, vol. 127, no. 3, pp. 1318–1327, 2010.
- [18] W. Hu, A. Abubakar, and T. M. Habashy, “Application of the nearly perfectly matched layer in acoustic wave modeling,” *Geophysics*, vol. 72, no. 5, pp. SM169–SM175, 2007.
- [19] B. Kaltenbacher, M. Kaltenbacher, and I. Sim, “A modified and stable version of a perfectly matched layer technique for the 3-d second order wave equation in time domain with an application to aeroacoustics,” *J. Comput. Phys.*, vol. 235, pp. 407–422, 2013.
- [20] H. Assi and R. S. C. Cobbold, “Perfectly matched layer for second-order time-domain elastic wave equation: formulation and stability,” *arXiv*, 2013.
- [21] —, “Compact second-order time-domain perfectly matched layer formulation for elastic wave propagation in two dimensions,” *Math. Mech. Solids*, 2015 (DOI: 10.1177/1081286515569266).
- [22] J. Lee and C. Shin, “Time-domain formulation of a perfectly matched layer for the second-order elastic wave equation with VTI media,” *J. Seism. Explor*, vol. 40, pp. 231–257, 2015.
- [23] M. A. Meyers and K. K. Chawla, *Mechanical Behavior of Materials*. New York: Cambridge University Press, 2008, ch. 2, Elasticity and Viscoelasticity, pp. 71-160.

- [24] H. T. Banks, S. Hu, and Z. R. Kenz, “A brief review of elasticity and viscoelasticity for solids,” *Adv. Appl. Math. Mech.*, vol. 3, no. 1, pp. 1–51, 2011.
- [25] J. Fang and Z. Wu, “Generalized perfectly matched layer for the absorption of propagating and evanescent waves in lossless and lossy media,” *IEEE Trans. Microwave Theory Tech.*, vol. 44, no. 12 Part 1, pp. 2216–2222, 1996.
- [26] J. Chung and G. M. Hulbert, “A time integration algorithm for structural dynamics with improved numerical dissipation: the generalized- α method,” *J. Appl. Mech.*, vol. 60, no. 2, pp. 371–375, 1993.
- [27] A. I. Beltzer, *Acoustics of solids*. New York: Springer-Verlag, 1988.
- [28] Y. Sumino, “The elastic constants of Mn_2SiO_4 , Fe_2SiO_4 and Co_2SiO_4 , and the elastic properties of olivine group minerals at high temperature.” *J. Phys. Earth*, vol. 27, no. 3, pp. 209–238, 1979.
- [29] J. D. Bass, D. J. Weidner, N. Hamaya, M. Ozima, and S. Akimoto, “Elasticity of the olivine and spinel polymorphs of Ni_2SiO_4 ,” *Phys. Chem. Minerals*, vol. 10, no. 6, pp. 261–272, 1984.
- [30] J. Bercoff, M. Tanter, M. Muller, and M. Fink, “The role of viscosity in the impulse diffraction field of elastic waves induced by the acoustic radiation force,” *IEEE Trans. Ultrason. Ferroelectr. Freq. Control*, vol. 51, no. 11, pp. 1523–1536, 2004.

Appendix A PML for viscoelastic media

It should be noted that the PML formulation presented in this paper models wave propagation in a loss-less media, for which, Hook's law as used in (1), is given by

$$\sigma_{ij} = \sum_{k,l=1}^3 C_{ijkl} \frac{\partial u_k}{\partial x_l}, \quad (23)$$

where σ_{ij} are the components of the symmetric stress tensor, and the components of the elasticity tensor, C_{ijkl} , are assumed to be real-valued. There are several different models that are used to account for viscous losses to the elastic wave equation [24]. One that is commonly used especially for modeling wave propagation in tissue [30], is the Kelvin–Vogit model, for which Hook's law takes the form

$$\sigma_{ij} = \sum_{k,l=1}^3 \left(C_{ijkl} + \eta_{ijkl} \frac{\partial}{\partial t} \right) \frac{\partial u_k}{\partial x_l}, \quad (24)$$

where η_{ijkl} is the viscosity tensor. For such a medium the wave equation is:

$$\rho \frac{\partial^2 u_i}{\partial t^2} = \sum_{j=1}^3 \frac{\partial}{\partial x_j} \left(\sum_{k,l=1}^3 C_{ijkl} \frac{\partial u_k}{\partial x_l} + \eta_{ijkl} \frac{\partial^2 u_k}{\partial t \partial x_l} \right). \quad (25)$$

Following the same steps used in deriving the elastic PML formulation in section 3, a PML formulation for the above viscoelastic wave equation can be obtained. The only difference, for this viscoelastic case, is that equation (13) in the derivation becomes:

$$\sum_{j=1}^3 \frac{\partial}{\partial x_j} \left(\sum_{k,l=1}^3 \frac{s_1 s_2 s_3}{s_j s_l} (C_{ijkl} - i\omega \eta_{ijkl}) \frac{\partial \hat{u}_k}{\partial x_l} \right). \quad (26)$$

This leads to the following PML formulation for the viscoelastic wave equation:

$$\rho_S \left(\frac{\partial^2 u_i}{\partial t^2} + a \frac{\partial u_i}{\partial t} + b u_i + c U_i \right) = \sum_{j=1}^3 \frac{\partial}{\partial x_j} \left(\sum_{k,l=1}^3 C_{ijkl} \frac{\partial u_k}{\partial x_l} + \eta_{ijkl} \frac{\partial^2 u_k}{\partial t \partial x_l} + w_{ij} \right) \quad (27a)$$

$$\frac{\partial w_{ij}}{\partial t} + \beta_j w_{ij} = \sum_{k,l=1}^3 \left(\tilde{\eta}_{ijkl} \frac{\partial^2 u_k}{\partial t \partial x_l} + (\tilde{C}_{ijkl} + \check{\eta}_{ijkl}) \frac{\partial u_k}{\partial x_l} + \check{C}_{ijkl} \frac{\partial U_k}{\partial x_l} \right) \quad (27b)$$

$$\frac{\partial U_i}{\partial t} = u_i, \quad (27c)$$

where $\tilde{\eta}_{ijkl}(\mathbf{x}) = (a - \beta_j - \beta_l) \eta_{ijkl}$, and $\check{\eta}_{ijkl}(\mathbf{x}) = (c / \beta_l) \eta_{ijkl}$, while the rest of the coefficients are as defined in elastic PML formulation as given in equation (18).